

Comparison of *In Situ* and Airborne Spectral Measurements of the Blue Shift Associated with Forest Decline

B. N. ROCK

Complex System Research Center, Institute for the Study of Earth, Oceans, and Space, University of New Hampshire, Durham, NH 03824

T. HOSHIZAKI

Geobotanical Remote Sensing Group, Jet Propulsion Laboratory, California Institute of Technology, Pasadena, California 91109

AND

J. R. MILLER

Department of Physics and Center for Research in Experimental Space Science, York University, North York, Ontario, M3J 1P3 Canada

During August 1985, extensive field activities were conducted at spruce/fir (*Picea* and *Abies*) sites in Vermont and Baden-Württemberg (FRG) currently undergoing rapid forest decline suspected of being due to various forms of air pollution. High-spectral resolution *in situ* reflectance curves and photosynthetic pigment determinations were acquired for common branch samples from specimens of spruce typical of both high- and low-damage sites. Similar spectral responses (reflectance data) were exhibited for specimens collected from high-damage sites in both the United States and FRG. Both current year and older foliage from high-damage sites in both countries showed an approximately 5 nm shift away from the normal inflection point of the red edge reflectance feature toward shorter wavelengths (a blue shift). This blue shift was associated with an observed reduction in chlorophyll b and a relative decrease in chlorophylls for needles collected from the high-damage sites, as compared with those from low-damage sites. An airborne high-resolution imaging spectrometer (the Fluorescence Line Imager or FLI) was flown over the Vermont study sites in August 1985 and has detected a blue shift of the chlorophyll absorption maximum at the high-damage site. Red edge parameters (wavelength position of the chlorophyll absorption maximum, red radiance, and NIR radiance) detected by the FLI have been used to image and map areas of damage in a highly accurate manner. Since data presented here suggest that the blue shift is a previsual symptom of damage, the ability to remotely detect such subtle spectral symptoms may serve as an early indicator of certain types of forest damage, and thus could be of considerable value in monitoring forest condition and state of health.

Introduction

Since the early 1960s, high elevation spruce-fir forests of the northeastern United States have undergone a marked decline in growth rate and state of health (Johnson and Siccama, 1984). During the same period, a similar decline in spruce, fir, and beech has been documented in many parts of central Europe (Schütt and Cowling, 1985). Developing a means of detecting, identifying, and quantifying

forest decline symptoms from orbital and/or airborne remote sensing platforms will provide scientists with the opportunity to assess, map, and monitor forest damage and decline on a global scale.

The stress agents responsible for the observed forest decline have not been identified, but various air pollutants, including acid deposition, ozone, and trace metals have been proposed (Friedland et al., 1984; Johnson and Siccama, 1984;

Vogelmann et al., 1985). Some of these stress agents may produce different physiological, anatomical and/or morphological symptoms which result in characteristic spectral expressions (Rock et al., 1986a,b). If so, such diagnostic spectral signatures could help identify specific kinds of damage caused by specific stress agents.

Recent studies of vegetation response to controlled application experiments in which tree seedlings have been exposed to known levels of pollutants, such as ozone, NO₂, SO₂, and artificial acid rain, suggest that initial, nonvisual effects occur which may involve a reductions in net photosynthesis. Some ozone-induced reductions in photosynthesis are directly related to declines in growth and yields (Reich and Amundson, 1985). Anatomical studies of tree seedlings exposed to known levels of pollutants indicate that a number of cellular-level changes (alteration of relative amounts of mesophyll cell to intercellular airspace volume, destruction of chloroplasts, build up of tannins, etc.) are induced (Crang and McQuattie, 1986), and these may have spectral expressions (Westman and Price, 1987). It should be noted that measured reductions in net photosynthesis and growth response are not well correlated with visible symptoms (Reich et al., 1984; 1986; Reich and Amundson, 1985; Reich and Lassoie, 1984; 1985), suggesting that spectral signatures related to nonvisual physiological and/or cellular damage may provide an early warning of great value in predicting growth declines.

Variation in chlorophyll and carotenoid concentrations, in addition to a buildup of additional pigments such as tannins, may occur within leaves in response to stress. Such pigment variations can be seen as spectral changes in specific por-

tions of reflectance curves acquired from vegetation subjected to various stress agents. Barber and co-workers (Horler et al., 1980; 1983) have related changes in the slope of the red edge (0.70–0.74 μm) to chlorophyll concentrations in the leaf. The position and slope of the red edge will change as healthy leaves progress from active photosynthesis through various stages of senescence (natural decline) due to loss of chlorophyll and the addition of tannins (Knippling, 1969).

A minor shift in the wavelength position of the red edge in green plant reflectance curves, to shorter wavelengths, is known as the blue shift and has been associated with heavy metal-induced stress in several vegetation types (Chang and Collins, 1983; Collins et al., 1981; 1983; Horler et al., 1980; 1983; Milton et al., 1983). An approximately 5 nm blue shift of the red edge has been detected in spruce specimens collected from high-damage sites in both Vermont and Baden-Württemberg (Rock et al., 1985; 1986a), and recent studies by Westman and Price (1987) suggest that pollutant treatment (ozone, SO₂, and acid misting) may cause this spectral feature in western conifers grown under controlled exposure conditions.

Satellite-borne remote sensing instruments such as the Multispectral Scanner (MSS) onboard Landsats 1–5 and the Thematic Mapper (TM) onboard Landsats 4 and 5 offer a unique perspective from which to study the Earth's vegetation. Such sensors provide a synoptic view of the Earth not available with standard aerial photography. In addition, the spectral coverage of the TM (0.4–2.4 μm) extends well out into the reflected infrared region of the electromagnetic spectrum (beyond 1.4 μm), a spectral region not covered by infrared-sensitive film and

an area in which canopy reflectance properties are affected by leaf moisture content (Gates, 1970; Goetz et al., 1983; Rohde and Olson, 1971; Tucker, 1980). One of the chief limitations of data acquired by the Landsat scanners is that due to coarse spectral resolution (between 100 and 200 nm wide spectral bandwidths), such sensors are unable to directly detect and identify surface materials characterized by subtle diagnostic spectral features such as the blue shift (Goetz et al., 1983; 1985).

Extended spectral coverage, coupled with the higher spectral resolution and improved radiometric sensitivity of orbital sensor systems planned for the 1990s [Moderate Resolution Imaging Spectrometer (MODIS) and High Resolution Imaging Spectrometer (HIRIS)], may allow scientists to detect and identify subtle but diagnostic spectral fine features associated with vegetation response to various stress agents. Thus, in addition to mapping and monitoring forest decline, future high-spectral resolution satellite systems may allow the discrimination of spectral "fingerprints," enabling investigators to identify specific types of forest damage.

In an attempt to develop understanding of the spectral properties associated with vegetation at various spatial scales (needles and leaves vs. canopies and communities) and its response to stress agents, appropriate ground-based analytical techniques must be developed which document the botanically significant spectral information that might be detected by sensors such as the TM, MODIS, and HIRIS. Studies which couple detailed ground spectral assessment with airborne high-spectral resolution sensors are an important part of research activities dedicated to the determination of those spec-

tral signatures which can be remotely detected by such sensor systems. This paper describes a study currently in progress at the Jet Propulsion Laboratory that uses intensive ground assessment data sets collected in conjunction with overflights by aircraft outfitted with advanced sensor systems.

Methods

Detailed ground assessments were conducted during August 1985, in conjunction with simultaneous aircraft overflights of study sites in both the United States (USA) and the Federal Republic of Germany (FRG). Study sites were selected which represent various levels of decline in spruce [*Picea rubens*, red spruce from Vermont (USA), and *Picea Abies*, Norway spruce from Baden-Württemberg (FRG)]. The Vermont study sites are located on Camels Hump Mountain in the central part of the Green Mountain Range, while the Baden-Württemberg sites are located in the northern Black Forest. For the Vermont study sites, additional ground data were collected in June 1985.

Aircraft overflights were made of the Vermont study sites with a high-spectral resolution imaging spectrometer known as the Fluorescence Line Imager (FLI), also known as the Programmable Multi-spectral Imager, manufactured and operated by Moniteq, Ltd.¹ of Toronto, under contract to the Department of Fisheries and Oceans, Canada (Hollinger et al., 1985). These flights were made on 4 August 1985, between 14:15 and 15:00

¹ The use of manufacturers names is done for clarity and does not constitute NASA endorsement of these products.

GMT, over several of the study sites on Camels Hump, VT. The FLI was also flown over several forest decline study sites in the FRG, including Baden-Württemberg, during the summer of 1986. Only FLI data acquired for the Camels Hump study will be described in this paper.

The FLI acquired data in its spectral mode in 288 contiguous bands in the spectral region from approximately 0.4 to 0.8 μm , providing a bandwidth of about 2.6 nm. Data were acquired at an altitude ranging from approximately 1000–1800 m above ground level, due to local variation in terrain. Pixel size in the spectral mode ranged from approximately 8×17 m at the high-damage site to 10×17 m for the low-damage site. Data from the FLI were recorded on a 14-track Bell and Howell M14L high density digital tape (HDDT) recorder.

Ground assessment included *in situ* spectral reflectance measurements acquired from samples of needles attached to branches representing separate age classes of needles on selected spruce trees, and laboratory analyses of photosynthetic pigments extracted from needles collected from the same branches. *In situ* spectral reflectance data were gathered for ground truth 25 June–5 July and 8–18 August 1985 for Vermont and 22–30 August 1985 for Baden-Württemberg. A high-spectral resolution spectrometer known as the VIRIS (Visible Infrared Intelligent Spectrometer), manufactured by Geophysical Environmental Resources, Inc.,¹ was used. The VIRIS acquires data in the 0.4–2.5 μm region at a bandwidth of from 2 nm in the 0.4–1.0 μm region, to 4 nm in the 1.0–2.5 μm region. Data are recorded on a digital tape cassette. A standardized setup is used to insure iden-

tical viewing conditions for all sample collections at each study site. Eight or more branch samples were collected at each site, and reflectance measurements were taken immediately thereafter using the sun as an illumination source. An approximately equal amount of leaf and branch material was used for each measurement. Measurements were made of needles attached to stems and arranged so that only a single-year's needles (current year, i.e., produced in 1985; 2-year-old, produced in 1984; and 3-year-old, produced in 1983, etc.) were in the field of view (approximately 1×3 cm) of the spectrometer. An attempt was made at each site to include branch samples which exhibited damage levels characteristic of the site. No defoliated branches or completely chlorotic needles were used.

Once field spectral measurements were acquired with the VIRIS, fresh needles (left on cut branches) were returned to JPL for pigment extraction and analysis. Branches were sealed in plastic bags containing moist paper towels, placed in coolers with ice, and shipped to California. Pigments were extracted from needles and analyses were conducted using standard procedures (Lichtenthaler and Wellburn, 1983). Absorption values were obtained at wavelengths of 0.470, 0.645, 0.662, and 0.710 μm to determine carotenoids and chlorophyll a and b content (Lichtenthaler and Wellburn, 1983; Wellburn and Lichtenthaler, 1982).

Results

In situ reflectance data

In situ reflectance curves of needles and branches collected from different spruce specimens show characteristic

spectral differences (Rock et al., 1985). Mean VIRIS reflectance data, ± 1 standard deviation from both a high- and low-damage site from Vermont illustrate these consistent differences (Fig. 1). Reflectance data collected in 1984 and 1985 from Vermont sites are very similar and the data in Fig. 1 are considered to be representative for the sites. The VIRIS data collected from the German sites in August of 1985 are presented in Fig. 2, and illustrate similar differences among damaged and undamaged foliage.

The spectral reflectance data presented in Figs. 1 and 2 were collected from mixed-age foliage on the most healthy trees occurring at a given site, and are therefore a conservative estimate of differences in the spectral properties of living branches and needles from high- and low-damage sites. There is a significant overlap in reflectance data from both countries in the visible portion of the spectrum, as well as at the longer wavelengths, beyond $1.4\ \mu\text{m}$, while little overlap occurs along the near infrared (NIR) plateau ($0.75\text{--}1.30\ \mu\text{m}$). The consistent reduced reflectance along the NIR plateau for those specimens collected from the high-damage sites may be related to the leaf biomass, cellular structure, and degree of hydration of leaf tissue (Gates, 1970; Rock et al., 1986b; Tucker, 1980), and suggests that a change in one or more of these leaf properties characterizes those specimens undergoing decline.

Averaged visible and near infrared VIRIS reflectance curves from Vermont specimens are presented in Fig. 3 and illustrates a shift in the red edge inflection point position for red spruce from high- and low-damage sites. The spectral data presented were acquired in August

1985 from 1-year old needles (produced in 1985) and indicate that some of the features described for Figs. 1 and 2, e.g., the reduced reflectance in the NIR, may not characterize new needles. Spectral data acquired in August 1985 of older needles do follow the patterns described for Figs. 1 and 2.

The slope and inflection point position of the red edge reflectance feature may be determined by calculating the first derivative of the spectral curve (Fig. 3). Wavelength positions of the red edge have been calculated for the August 1985 VIRIS data collected from Vermont and are summarized in Table 1. A distinctive blue shift, defined here as a shift of the red edge inflection point to shorter wavelengths, is seen in reflectance data from samples collected at the high-damage sites for both current year and older needles. Changes in the position of the red edge were evaluated using analysis of variance. This analysis suggests that for the Vermont data there are characteristic differences for individual sites which are highly significant.

Extensive *in situ* spectral data gathered during August of 1985 on the wavelength position of such features as the chlorophyll absorption maximum and red edge inflection point (Table 1) suggest that a shift in position of chlorophyll absorption maximum may not be a consistent feature extractable from VIRIS spectral data from high- and low-damage sites. These data indicate that a shift in wavelength position of the chlorophyll absorption feature, although highly significant ($p < 0.001$) for 1983 needles, is very minor (approximately 1 nm) and in the longer wavelength direction. The approximately 5 nm red edge shift, however, is distinctive. Similar red edge inflection point shifts are

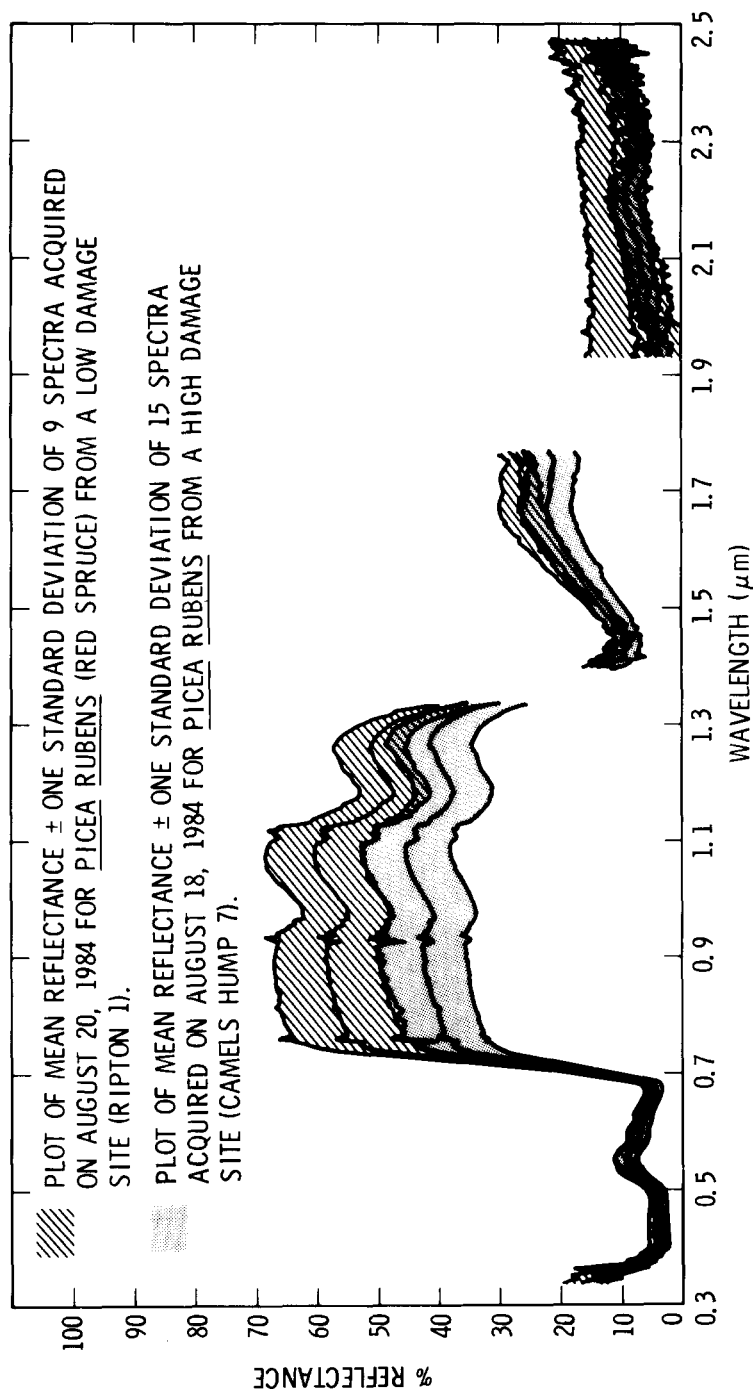


FIGURE 1. Field reflectance curves of *Picea rubens* from a high- and a low-damage site in Vermont (Taken from Rock et al., 1985).

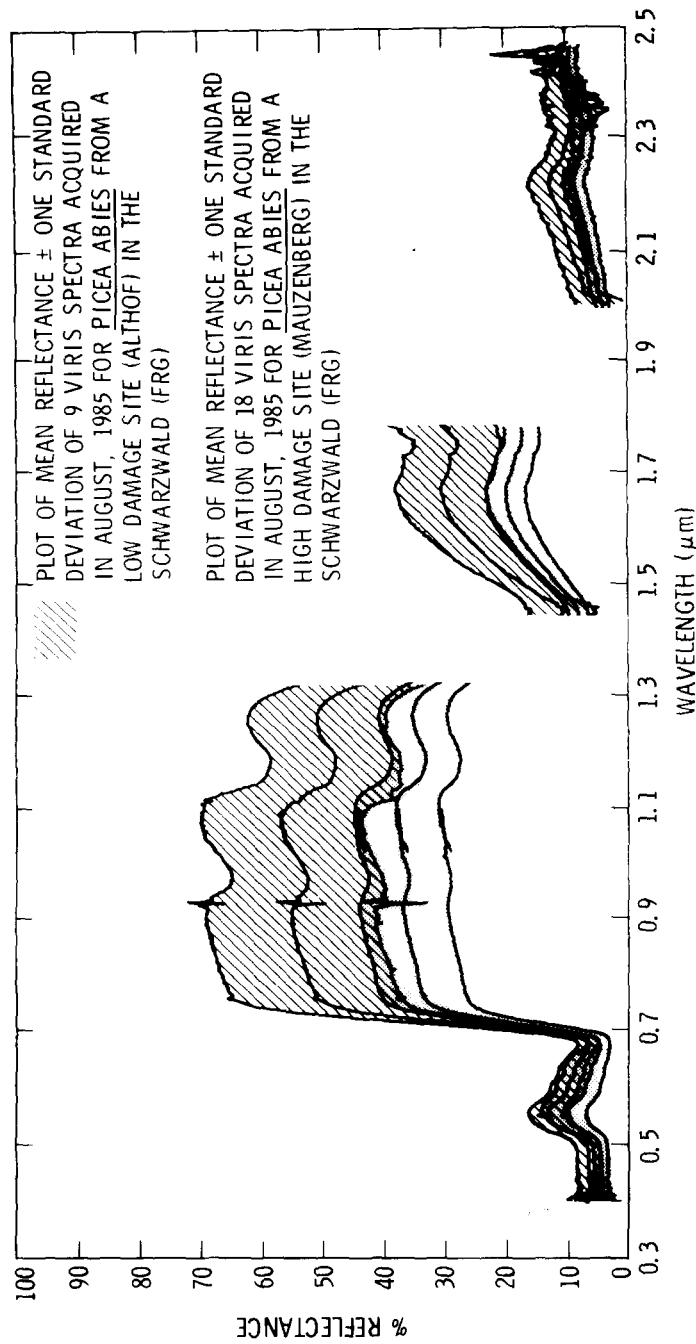


FIGURE 2. Field reflectance curves of *Picea Abies* from a high- and a low-damage site in Germany (Modified from Rock et al., 1986a).

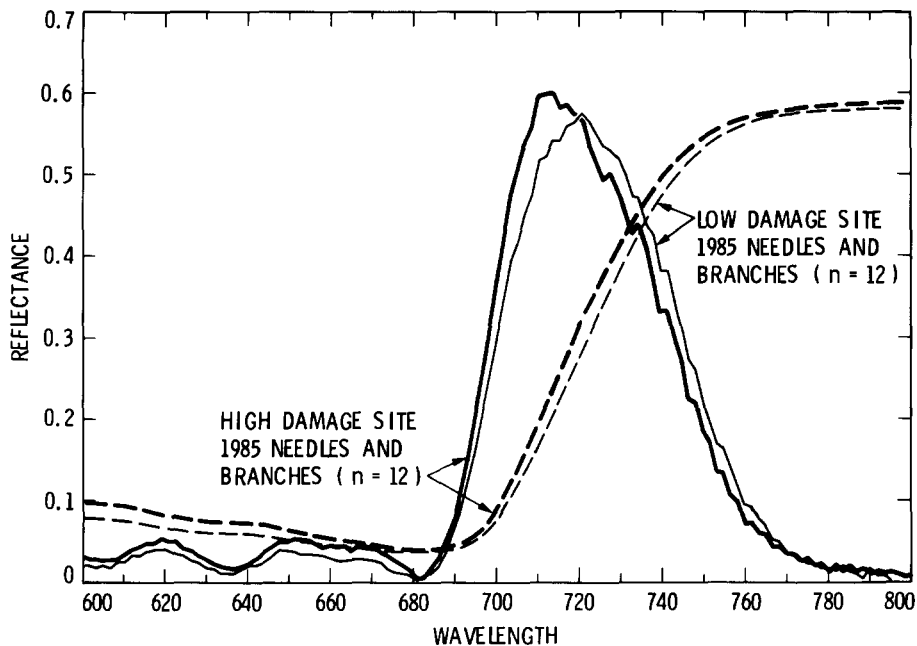


FIGURE 3. Comparison of averaged VIRIS reflectance curves (dashed lines) for plants from a high- and a low-damaged site in Vermont. First derivative curves of each spectrum are presented as solid lines. Data were collected in June, 1985.

also seen in VIRIS reflectance data from Baden-Württemberg (Table 2).

Pigment data

For 3-year old (1983) needles from Vermont, total amounts of chlorophyll a and b and the ratio of total chlorophyll (a+b) to total carotenoid were significantly lower in needles collected in

August from high-damage sites while the ratio of chlorophyll a to b was found to be significantly greater in high-damage site samples (Fig. 4). Chlorophyll b content was relatively low when compared to chlorophyll a in damaged spruce needles from both countries. Results indicate that in spruce needles, stress factors decrease the amount of chlorophyll b the most, followed by chlorophyll a, with the least

TABLE 1 VIRIS Spectral Data of 1985 and 1983 Needles from Red Spruce Growing in Low- and High-Damage Sites Obtained in August 1985 from Camels Hump, Vermont^a

VERMONT STUDY SITES	n	SELECTED VIRIS SPECTRAL PARAMETERS		
		CHLOROPHYLL WELL (nm)	RED EDGE INFLECTION POINT (nm)	MSI VALUES ($\frac{1630-1660 \text{ nm}}{1230-1270 \text{ nm}}$)
Low damage (1985 needles)	12	679.87 \pm 1.01 ^{NS}	719.37 \pm 3.19 ^{***}	0.477 \pm 0.029 ^{**}
High damage (1985 needles)	12	680.60 \pm 0.97	714.17 \pm 2.88	0.509 \pm 0.024
Low damage (1983 needles)	11	679.59 \pm 0.85 ^{***}	721.00 \pm 2.07 [*]	0.545 \pm 0.034 ^{**}
High damage (1983 needles)	11	680.93 \pm 0.64	716.70 \pm 5.19	0.600 \pm 0.039

^aData are presented as the mean \pm 1 standard deviation: n = number of samples, nm = nanometer, MSI = moisture stress index, NS = not significantly different, * = $P < 0.02$, ** = $P < 0.01$, *** = $P < 0.001$. 1985 needles emerged in 1985, 1983 needles in 1983.

TABLE 2 Mean Red Edge Position for VIRIS Data Acquired in August 1985 from Vermont (VT) and Baden-Württemberg (BW) Spruce Specimens^a

SITES	n	RED EDGE INFLECTION POINT (nm)			
		1985 NEEDLES	n	1983 NEEDLES	
VT low damage	12	719.4 ± 3.19***	11	721.0 ± 2.07*	
VT high damage	12	714.2 ± 2.88	11	716.7 ± 5.19	
BW low damage	8	722.8 ± 2.24**	8	721.8 ± 2.82*	
BW high damage	8	717.5 ± 4.05	8	714.4 ± 8.29	

^aData are presented as the mean ± 1 standard deviation: n = number of samples, nm = nanometer, * = $P < 0.02$, ** = $P < 0.01$, *** = $P < 0.001$. See also Table 1.

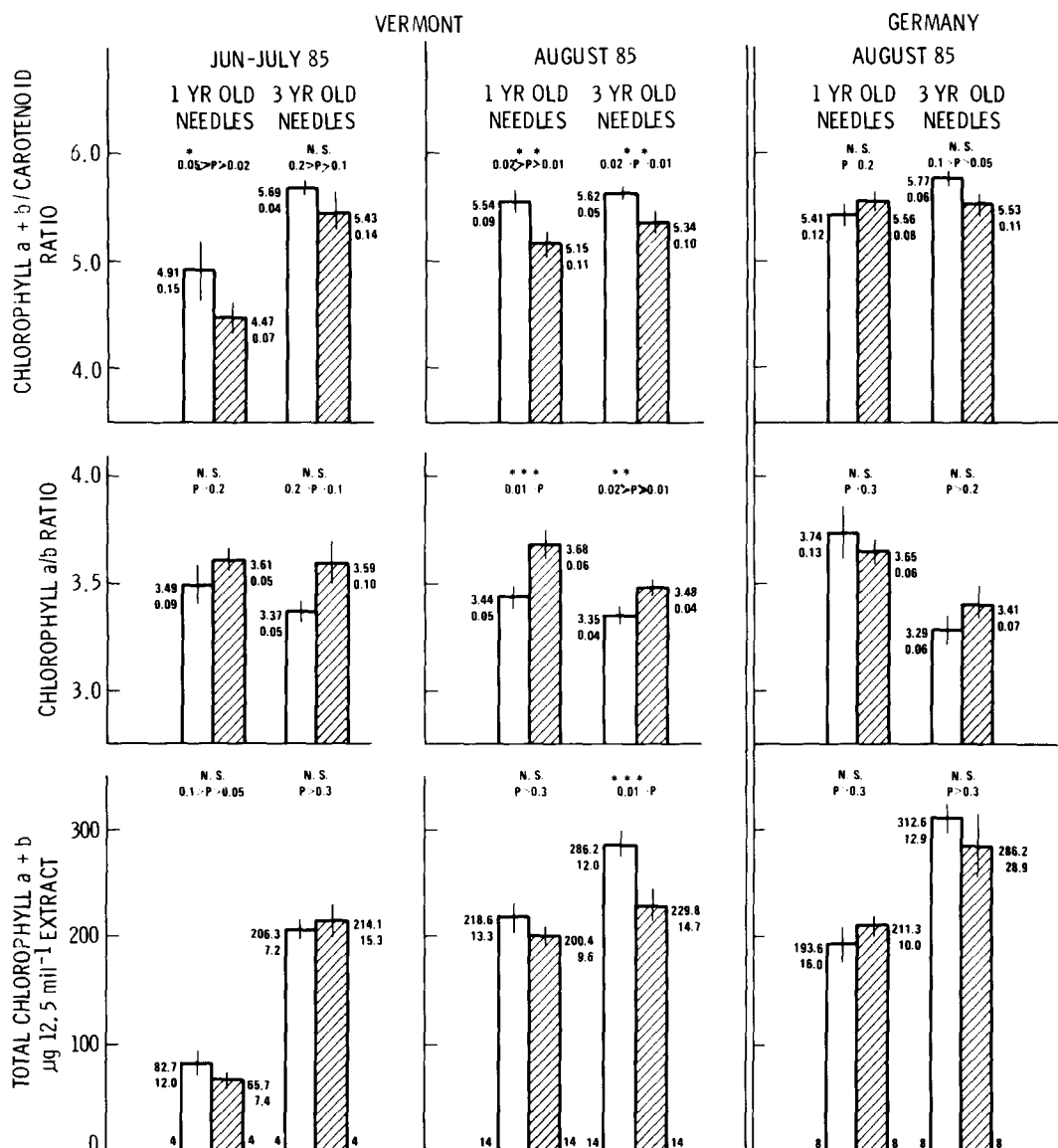


FIGURE 4. Effects of stress and seasonality on pigment concentrations and ratios for one-year-old and three-year-old needles from red spruce (Vermont) and Norway spruce (Germany). Open columns represent data from low-damage specimens and cross-hatched columns from high-damage specimens. One-year-old needles emerged in 1985 and three-year-old in 1983. Samples were harvested in June, July and August 1985. Mean values next to bar top with one standard error value below.

amount of change seen in carotenoid pigments (Rock et al., 1986a, b).

Samples of 1-year- (1985) and 3-year old (1983) needles were harvested at the beginning (June) and the end (August) of the 1985 growing season in Vermont to determine pigment conditions which might be related to seasonal differences. Differences in pigments values for the high- and low-damage sites were more pronounced in late summer than in early summer (Fig. 4).

Samples of 3-year-old (1983) Norway spruce needles were gathered in Germany near the midpoint of their growing season (late August 1985). Results similar to 3-year-old needles of the Vermont red spruce were obtained (Fig. 4). Pigment data from 1-year-old needles (1985) of Norway spruce were found to be highly variable. Only trends (not statistically significant) for the third year needles could be suggested and no conclusion as to the differentiation of low- and high-damage sites could be drawn from these data sets from Germany.

Fluorescence line imager (FLI) data

The data presented here were acquired from a single flightline (Plate IX) selected so as to include both the lowest damage site on Camels Hump (site #1, with approximately 12% spruce damage, 4% spruce mortality, as determined by ground assessment; Rock et al., 1985; Vogelmann and Rock, 1986) as well as the highest damage site (site #7, with approximately 76% spruce damage, 24% spruce mortality). Raw FLI data acquired during this single overpass are presented in Plate X(a); in which the relative spectral radiance curves are plotted for three pixels selected from within the high-damage site and four pixels from within the low-damage site. These same data are

shown in Plate X(b) after a normalization procedure was applied which is intended to visually accentuate spectral differences along the red edge for spectra with varying reflectance shoulder excursions. Using this approach, the maximum signal (on the reflectance infrared shoulder) and the minimum signal (in the chlorophyll absorption maximum) are normalized to unity and to zero, respectively, for each FLI spectrum being compared. This presentation illustrates the consistency in spectral shape that was observed for pixels in each of the particular damage sites and it also illustrates a systematic "blue shift" of the red edge for the high-damage pixel spectra relative to the low-damage pixel spectra.

A multistep image analysis procedure was used to provide a quantitative description of the FLI data in the red edge spectral region ($0.67\text{--}0.80\ \mu\text{m}$). The raw pixel spectra [e.g., Plate X(a)] are converted to pseudoreflectances by applying the radiometric calibration data and then dividing by a standard extraterrestrial solar irradiance spectrum (Thekekar, 1974). Those spectral regions affected by atmospheric absorption are then masked, and the remaining spectral data are fitted with an inverted Gaussian model for the vegetation red edge (Miller et al., 1985). The derived model parameters are i) the infrared shoulder reflectance (R_s), ii) the reflectance minimum corresponding to the chlorophyll absorption maximum (R_0), iii) the wavelength (λ_0) at the reflectance minimum, and iv) the red edge inflection point wavelength (λ_p). The above analysis for spectra from within the high-damage and low-damage areas from Camels Hump yielded the red edge reflectance parameter values indicated in Table 3. Quantitative red edge analysis of selected FLI spectra resulted in red edge

TABLE 3 FLI Spectral Data Acquired 4, August 1985 for High- (Site #7—Plate IX) and Low-Damage (Site #1—PlateIX) Sites on Camels Hump Mountain, Vermont^a

SELECTED FLI SPECTRAL PARAMETERS					
VERMONT STUDY SITES	n	CHLOROPHYLL WELL REFLECTANCE (R_0)	NIR SHOULDER REFLECTANCE (R_s)	CHLOROPHYLL WELL (nm)	RED EDGE INFLECTION POINT (nm)
Low damage	4	$0.042 \pm 0.003^{***}$	$0.452 \pm 0.015^{***}$	$685.7 \pm 0.52^{***}$	715.1 ± 1.1^{NS}
High damage	3	0.062 ± 0.005	0.377 ± 0.035	681.1 ± 1.1	714.1 ± 0.83

^aData are presented as the mean \pm 1 standard deviation: n = number of samples, NS = not significantly different, *** = $P < 0.001$.

model reflectance curves shown in Fig. 5 for four pixels in the high-damage and the two in low-damage sites.

A color composite image of potential vegetation damage based on modeled red

edge parameters detected by the FLI is presented in Plate XI. This image, represented by a combination of the minimum reflectance (R_0 , color-coded blue), the shoulder of the NIR reflectance (R_s ,

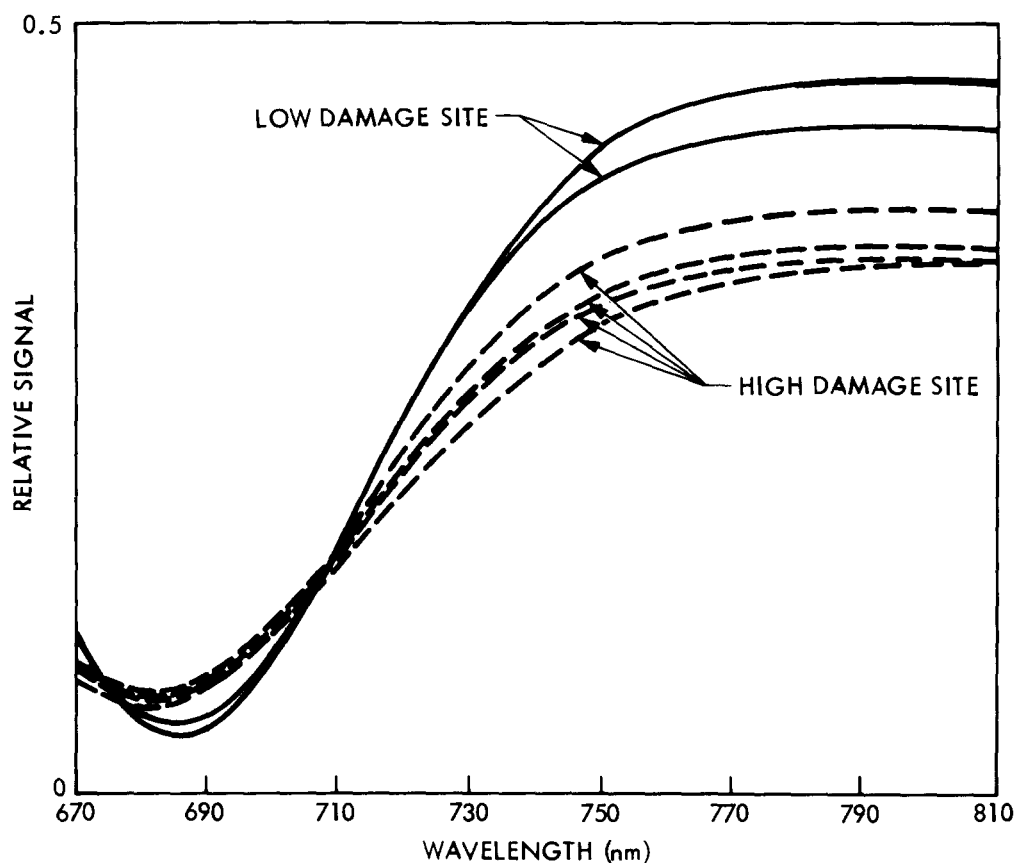


FIGURE 5. Comparison of the modeled red edge reflectance spectra developed through a multistep image analysis procedure for the high-damage and low-damage sites. See also Table 3 for the red edge reflectance parameter values.

color-coded green), and the wavelength position of the chlorophyll absorption maximum (λ_0 , color-coded red) derived from the FLI spectral data, is compared with a Thematic Mapper Simulator (TMS) image utilizing two spectral bands and a band ratio which mimics the moisture stress index, as described elsewhere (Rock et al., 1986b). The TMS image has been shown to be an extremely accurate map of damage levels on Camels Hump (Vogelmann and Rock, 1986).

Discussion

In situ VIRIS reflectance data from both the USA and FRG (Figs. 1, 2, and 3; Table 1) are very similar, with the most obvious similarities noted in the relative change in reflectance values for the NIR spectral region, the strong inverse correlation between NIR reflectance and visual damage levels and the occurrence of the blue shift in specimens from high-damage sites. Similar differences are also seen in the calculated moisture stress index (MSI) ratio that has proved useful as a means of mapping forest decline damage using TM/TMS data (Rock et al., 1986b; Vogelmann and Rock, 1986; 1987a).

The NIR reflectance variables suggest that a range of cellular and/or biomass variations are associated with damage levels. Since an effort was made to include equal amounts of needle and branch material in the field of view of the VIRIS, it is felt that some of the NIR reflectance variation is due to some factor other than differences in biomass. Anatomical assessment of needles collected in Vermont indicate that cellular damage does characterize mesophyll tissue of needles from high-damage sites (Rock et al., 1986b; Vogelmann and Rock, 1987b). The greater

range of variation seen in the NIR reflectance for the low-damage site in Baden-Württemberg is likely an indication of the greater range of cellular damage that characterizes even low-damage sites in the Black Forest.

The blue shift of the red edge seen in VIRIS spectra acquired for species from high-damage sites in both Vermont and Baden-Württemberg is a consistent spectral feature associated with damage in spruce needles attached to branches. Helicopter-borne spectrometer data, gathered in August 1984 (Rock et al., 1985), and the FLI data presented in this paper support the view that a shift to shorter wavelengths of the chlorophyll maximum absorption feature may also characterize the canopy of spruce forests undergoing decline. However, the data presented in Fig. 3 and Table 1 suggest that a shift in the position of the red edge need not be accompanied by a similar shift in position of the chlorophyll maximum absorption features. *In situ* spectral data gathered in Vermont suggest, instead, that, independent of the wavelength position of the chlorophyll feature, the width of the chlorophyll absorption maximum also influences the position of the red edge.

It is a well-known property of absorption by atmospheric gases that as the concentration of a gas increases, the width of the absorption band or line increases, a phenomenon known as line broadening (Goody, 1964; Howard et al., 1955). In reverse, as concentration of an absorption medium decreases, the width of the absorption feature also decreases. It is reasonable to assume that as total chlorophyll concentration decreases, the position of the red edge would move to shorter wavelengths as the width of the chlorophyll absorption feature narrows. If chlo-

rophyll concentrations in healthy needles is above the point of saturation, i.e., above the concentration beyond which the field spectrometer is unable to monitor increases, minor decreases in chlorophyll concentrations associated with increasing damage could lead first to a narrowing of the chlorophyll well, followed by increasing reflectance at the wavelength of maximum absorption. In such a manner, a blue shift of the red edge could occur independent of a change in the position of the chlorophyll absorption maximum. Measured decreases in total chlorophyll reported here suggests that the blue shift seen in 1985 VIRIS data may be due to such a reversed line broadening phenomenon.

An alternative explanation regarding the possible cause of the blue shift of the red edge has been provided by Lichtenthaler and co-workers. Experimental results suggest that fluorescence associated with initial damage to the photosynthetic apparatus may account, at least in part, for the blue shift phenomenon (Lichtenthaler and Buschmann, 1987).

An examination of data presented in Table 1 suggests that the blue shift of the red edge is characteristic in both 1985 needles and 1983 needles from high-damage sites, and is on average a shift of approximately 5 nm to shorter wavelengths. The higher standard deviations associated with red edge position data for 1983 needles from high-damage sites (Table 2) suggests a higher degree of variability of damage, especially in the Black Forest. Pigment data (Fig. 4) from damage sites in Germany also suggests the same high degree of variability. It should be noted that the occurrence of the blue shift in green (nonchlorotic) 1985 and 1983 spruce needles from apparently

healthy specimens growing at the high-damage site in Vermont suggests that such a shift represents a previsual or nonvisual spectral indicator of forest decline stress.

In situ reflectance data for the visible region (Fig. 2) suggests that greater variability in this region characterizes both high- and low-damage sites in Germany. The strong chlorosis which characterizes forest decline at both high- and low-damage sites in the Black Forest reinforces such observations. Chlorosis was not a striking visual characteristic of forest decline damage in Vermont in 1984. The lack of chlorosis, even at high-damage sites characterized by extensive needle loss, is emphasized by the nearly total overlap and narrow variability seen in the visible 1984 spectral data presented in Fig. 1.

Blue shifts of the red edge have been reported in various types of vegetation growing in soils high in trace metals (Collins et al., 1981; 1983; Milton et al., 1983); the appearance of such a spectral shift in the reflectance data acquired for spruce from high-damage sites in Vermont and Baden-Württemberg suggests that trace metal stress to vegetation may be a factor in the forest decline at both sites. However, since we know little regarding the subtle spectral properties associated with damage induced by other forms of stress factors (i.e., ozone, acid rain, etc.) it is premature to infer potential causal agents of decline on the basis of spectral data. Studies must be designed similar to those reported by Westman and Price (1987) in which a spectral analysis is included as part of the harvest activities conducted for controlled exposure experiments.

The photosynthetic pigment data (Fig. 4) for older needles from both Vermont and Baden-Württemberg show very simi-

lar trends: In response to increasing damage, total chlorophyll concentrations decrease, chlorophyll to carotenoid ratios decrease, and chlorophyll a to b ratios increase. Thus it is clear that alteration of kinds and amounts of pigments occurs in response to increasing damage levels in both countries, and is likely related to reductions in net photosynthesis and growth response.

In general, the various pigment values from the Vermont study sites were not significantly different at the beginning of the season but were significantly different by the end of the growing season, thus indicating a damaged condition had developed between June and August in needles obtained from the high-damage site. The data agree well with anatomical assessments conducted on needles from the same branches used for pigment analysis (Rock et al., 1986b; Vogelmann and Rock, 1987b). In that study, the number of damaged cells in needles from the high damage site was found to be greater in late summer. Both of these data sets support the view that stress factors involved in the forest decline phenomenon exert a strong influence during the summer months.

The FLI spectral curve data presented in Plate X and Fig. 5 are similar to VIRIS reflectance curve data acquired for the 0.4–0.8 μm spectral region (note Figs. 1 and 2). This is encouraging since the VIRIS is gathering reflectance data from only 1×3 cm area of spruce needles and branch material while the FLI gathers data from a canopy area approximately 10×17 m, containing spruce and fir materials, as well as broadleaf understory and ground cover components.

In the visible region, the FLI data show an increased brightness in the green peak

region (0.5–0.6 μm) and in the chlorophyll maximum absorption region (0.65–0.7 μm) [see Table 3 and Plate X(a)], suggesting some chlorosis may be symptomatic of the high-damage site in 1985. Based on visual field assessment, chlorosis was not recognized as a symptom at the high-damage site on Camels Hump in the summer of 1984 (note Fig. 1), whereas it was noted as occurring in some trees at the high-damage site in 1985. The FLI spectral data support the view that chlorosis is a visible symptom characterizing the high damage site (Plate XI).

The blue shift of the red edge is clearly visible in the FLI pixel data acquired from the high-damage site [Plate X(b)]. A quantitative comparison of the low-damage to high-damage site spectral properties of the red edge, however, fails to reveal a statistically significant blue shift in the red edge inflection point position (Table 3). This is in contrast to the data acquired with the VIRIS (Table 1). Further comparison of FLI and VIRIS data indicate differences in the wavelength position of the chlorophyll absorption maximum between these data sets for high- and low-damage sites. The significance of this fact is not clear. It should be noted that the wavelength of the red edge inflection point is not derived in the same way for the VIRIS as for the FLI spectra. For the VIRIS the inflection point represents the maximum in the reflectance first derivative curve as previously discussed; however, for the FLI spectra the presence of the atmospheric absorption features makes this approach impossible, so that the inflection point wavelength is that derived from the best-fit inverted Gaussian model curve.

The FLI radiance and pseudo-reflectance data in the 0.75–0.8 μm [Plate X(a)]

and Fig. 5] spectral region indicate a relative decrease in the NIR shoulder reflectance in the high-damage spectra when compared to the low-damage spectra. This is in good agreement with the VIRIS *in situ* data (Fig. 1). This result is of particular interest since the reflectance data gathered by NASA helicopter in a previous study (Rock et al., 1985) suggested that whole canopy reflectance values in the NIR from the high-damage sites might be higher than those from low-damage sites. Further study of the NIR reflectance properties of spruce canopies undergoing decline is needed.

It is interesting to speculate about the optical effect on the airborne imagery of the high spruce mortality (24%) in the high-damage site with the associated exposed branches and bark. In mixed-pixel simulations of the expected composite reflectance spectra resulting from combining varying fractions of bark and needle spectra for black spruce, it was found that reduced amounts of needle spectra effected a blue shift of the chlorophyll well position with a much smaller blue shift of the red edge position. In addition, increasing the bark spectral contribution resulted in visible reflectance increase and NIR reflectance decreases which are in agreement with our field measurements and those of others (e.g., Teillet et al., 1985). If this black spruce simulation is used to explain the observed blue shift of 5 nm in the chlorophyll absorption maximum wavelength position in FLI data, a bark spectrum composition of 55% would be required (relative to pure needle spectra) which would then also infer a red edge position blue shift of 0.2 nm, an increase in the chlorophyll well reflectance by a factor of 1.6 and a decrease in the shoulder reflectance by a factor of

0.75. These observations are generally consistent with the differences observed in the FLI spectral data from the high-damage and low-damage sites, therefore providing a possible alternative interpretation of the blue shift observations in the FLI data. However, our field surveys (Rock et al., 1985; Vogelmann and Rock, 1986) do not support the suggestion of such a large fractional contribution by bark spectra.

The color composite of vegetation damage (Plate XI), derived from the FLI spectral data, correlates remarkably well with damage areas identified in the accompanying TMS image. Both images depict a spatial distribution of damage which corresponds very well with known ground conditions. The FLI image relied heavily on the wavelength position of the chlorophyll maximum absorption feature while the TMS image relies on the ratio of shortwave IR bands for the detection and mapping of damage (Rock et al., 1986b). At this point it is not clear what canopy parameters are being measured by either the FLI or the TMS approaches. The fact that both images depict areas of known damage with a high degree of accuracy suggests that both approaches are detecting some aspects of the canopy associated with forest decline damage. Further study is required before a statement can be made regarding the actual biophysical canopy property or properties being detected by either instrument.

Summary

In situ VIRIS (Visible Infrared Intelligent Spectrometer) reflectance data were found to have characteristic features cor-

related with visual forest decline damage in *Picea rubens*, red spruce of Vermont and *Picea Abies*, Norway spruce of Baden-Württemberg. These spectral characteristics are very similar in the two species and suggest that similar kinds of damage occur in each.

VIRIS spectra of both species from high-damage sites include a 5 nm shift of the red edge inflection point to the shorter wavelength (a blue shift) and a decrease in the reflectance of the near infrared plateau (0.75–1.30 μm). *In situ* reflectance data from Vermont fails to show a blue shift of similar magnitude for the chlorophyll absorption maximum. In the Vermont data, the red edge shift constitutes a previsual indicator of stress and/or damage. Pigment data for both species indicate that a loss of total chlorophylls, an increase in chlorophyll a to b ratio, and a decrease in chlorophyll to carotenoid ratio are associated with the red edge shift.

Spectral data from the airborne Fluorescence Line Imager (FLI) was similar to but not identical with the *in situ* VIRIS data. FLI spectral features characteristic of the high-damage site were a blue shift of the chlorophyll absorbance maximum, a decrease in the reflectance in the NIR plateau, and an increase in reflectance in the visible red. A blue shift of the red edge was seen in normalized FLI spectral data but an analysis of modeled red edge data failed to demonstrate a statistically significant shift in wavelength position.

The characteristic blue shift of the chlorophyll absorption maximum, as well as the increased red radiance and decreased NIR radiance for damaged spruce may be used to delineate and map damage areas on Camels Hump with FLI data. The resulting map agrees well with known

areas of damage (based on detailed ground assessment) and with TMS imagery.

Comparison of the FLI data with mixed-pixel simulations of expected composite reflectance spectra suggests that the red edge parameters detected by the instrument may be related to percent mortality and foliar loss characterizing a given site, rather than pigment and cellular changes associated with forest decline damage as detected by *in situ* measurements.

The research described in this paper was carried out at the Jet Propulsion Laboratory, California Institute of Technology, under contract with the National Aeronautics and Space Administration. We wish to acknowledge the contributions of the following people to various portions of this study: Drs. H. W. Vogelmann, H. Lichtenthaler, J. E. Vogelmann and W. Berry and D. L. Williams, G. Schmuck and S. Wong. With respect to FLI data reported here the authors wish to acknowledge the dedication and persistence of Lawrence Gray (Moniteq, Ltd.) who made FLI spectral mode data available over Camels Hump, Don Sturgeon and Doug Dunlop (Moniteq, Ltd.) who contributed in the development of FLI analysis software and Ed Hare (York University) who calculated the inverted-Gaussian model.

References

- Chang, S. H., and Collins, W. (1983), Confirmation of the airborne biogeophysical mineral exploration technique using laboratory methods, *Econ. Geol.* 78:723–736.
- Collins, W., Chang, S. H., and Kus, J. T. (1981), Detection of hidden mineral de-

- posits by airborne spectral analysis of forest canopies, NASA Contract NSG-5222, Final Report, 61 pp.
- Collins, W., Chang, S. H., Raines, G., Canney F., and Ashley, F. (1983), Airborne biogeochemical mapping of hidden mineral deposits, *Econ. Geol.* 78:737-749.
- Crang, R. E., and McQuattie, C. J. (1986), Qualitative and quantitative effects of acid misting and two air pollutants on foliar structures of *Liriodendron tulipifera*, *Can. J. Bot.* 64:1237-1243.
- Friedland, A. J., Johnson, A. H., and Siccama, T. G. (1984), Trace metal content of the forest floor in the Green Mountains of Vermont: spatial and temporal patterns, *Water, Air, Soil Pollution* 21:161-170.
- Gates, D. M. (1970), Physical and physiological properties of plants, In *Remote Sensing With Special Reference to Agriculture and Forestry*, National Academy of Science, Washington, DC, pp. 224-252.
- Goetz, A. F. H., Rock, B. N., and Rowan, L. C. (1983), Remote sensing for exploration: An overview, *Econ. Geol.* 78:573-590.
- Goetz, A. F. H., Vane, G., Solomon, J. E., and Rock, B. N. (1985), Imaging spectrometry for Earth remote sensing, *Science* 228: 1147-1153.
- Goody, R. M. (1964), *Atmospheric Radiation: I, Theoretical Basis*, Oxford University Press, Oxford, 436 pp.
- Hollinger, A. B., O'Neill, N. T., Dunlop, L. D., Cooper, M. T., Edel, H., and Gower, J. F. R. (1985), Water-depth measurement and bottom type analysis using a two-dimensional array imager, In *Proceedings of the Nineteenth International Symposium on Remote Sensing of Environment*, Ann Arbor, Michigan, 21-25 October.
- Horler, D. N. H., Barber, J. and Barringer, A. R. (1980), Effects of heavy metals on the absorbance and reflectance spectra of plants, *Int. J. Remote Sens.* 1:121-136.
- Horler, D. N. H., Dockray, M., Barber, J., and Barringer, A. R. (1983), Red edge measurements for remotely sensing plant chlorophyll content, *Committee on Space Research Symposium On Remote Sensing and Mineral Exploration Proceedings*, Pergamon, Oxford, Vol. 3, pp. 273-277.
- Howard, J. N., Burch, D. L., and Williams, D. (1955), Near-infrared transmission through synthetic atmospheres, *Geophysical Research Papers* No. 40, Air Force Cambridge Research Center, Bedford, MA, 244 pp.
- Johnson, A. H., and Siccama, T. C. (1984), Decline of red spruce in the northern Appalachians: assessing the possible role of acid deposition, *Tappi J.* 67:68-72.
- Knipling, E. B. (1969), Leaf reflectance and image formation on color infrared film. In *Remote Sensing in Ecology* (P. L. Johnson, Ed.), Univ. of Georgia Press, Athens, pp. 17-29.
- Lichtenthaler, H. K., and Buschmann, C. (1987), Reflectance and chlorophyll fluorescence signatures of leaves, In *Proceeding of the International Geoscience and Remote Sensing Symposium (IGARSS '87)*, IEEE 87CH2434-9, IEEE, New York, Vol. 2, pp. 1201-1206.
- Lichtenthaler, H. K., and Wellburn, A. R. (1983), Determination of total carotenoids and chlorophyll a and b of leaf extracts in different solvents, *Biochem. Soc. Trans.* 603:591-592.
- Miller, J. R., Hare, E. W., Neville, R. A., Gauthier, R. P., McColl, W. D., and Till, S. M. (1985), Correlation of metal concentration with anomalies in narrow band multispectral imagery of the vegetation red reflectance edge, In *Proceedings of the International Symposium on Remote Sensing of the Environment. Fourth Thematic Conference, Remote Sensing for Exploration Geology*, San Francisco, April, pp. 143-154.
- Milton, N. M., Collins, W., Chang, S. H., and Schmidt, R. G. (1983), Remote detection of metal anomalies on Pilot Mountain,

- Randolph County, North Carolina, *Econ. Geol.* 78:605–617.
- Reich, P. B., and Amundson, R. G. (1985), Ambient levels of ozone reduce net photosynthesis in tree and crop species, *Science* 230:566–570.
- Reich, P. B., and Lassoie, J. P. (1984), Effects of low level ozone exposure on leaf diffusive conductance and water-use efficiency in hybrid poplar, *Plant, Cell Environ.* 7:661–668.
- Reich, P. B., and Lassoie, J. P. (1985), Influence of low concentrations of ozone on growth, biomass partitioning and leaf senescence in young hybrid poplar plants, *Environ. Pollution* 39:39–51.
- Reich, P. B., Lassoie, J. P., and Amundson, R. G. (1984), Reduction in growth of hybrid poplar following field exposure to low levels of O₃ and (or) SO₂, *Can. J. Bot.* 62:2835–2841.
- Reich, P. B., Schoettle, A. W., and Amundson, R. G. (1986), Effects of O₃ and acid rain on photosynthesis and growth in sugar maple and northern red oak seedlings, *Environ. Pollution* 40:1–15.
- Rencz, A. N., Bonham-Carter, G. F., van der Greint, C., Miller, J. R., and Hare, E. W. (1986), Preliminary results from modeling vegetation spectra derived from MEIS data, Algonquin Park, Ontario, In *Proceedings of the 10th Canadian Symposium on Remote Sensing*, Edmonton, forthcoming.
- Rock, B. N., Williams, D. L., and Vogelmann, J. E. (1985), Field and airborne spectral characterization of suspected acid deposition damage in red spruce (*Picea rubens*) from Vermont, In *1985 Machine Processing of Remotely Sensed Data Symposium*, LARS/Purdue, W. Lafayette, IN, pp. 71–81.
- Rock, B. N., Hoshizaki, T., Lichtenthaler, H. and Schmuck, G. (1986a), Comparison of *in situ* spectral measurements of forest decline symptoms in Vermont (USA) and the Schwarzwald (FRG), In *Proceedings of the International Geophysical and Remote Sensing Symposium (IGARSS '86)*, IEEE 86CH2268-1, IEEE, New York, Vol. 3, pp. 1667–1672.
- Rock, B. N., Vogelmann, J. E., Williams, D. L., Vogelmann, A. F., and Hoshizaki, T. (1986b), Remote detection of forest damage, *BioScience* 36:439–445.
- Rohde, W. G., and Olson, C. E., Jr. (1971), Estimating foliar moisture content from infrared reflectance data, In *Third Biennial Workshop, Color Serial Photography in the Plant Sciences*, American Society of Photogrammetry, Falls Church, VA, pp. 144–164.
- Schütt, P., and Cowling, E. B. (1985), Waldsterben, a general decline: symptoms, development, *Plant Dis.* 69:548–558.
- Teillet, P. M., Leckle, D. G., Ostaff, D., Fedosejevs, G., and Ahearn, F. J. (1985), Spectral measurements of tree defoliation, In *Proceedings of the 3rd International Colloquium on Spectral Signatures of Objects in Remote Sensing*, Les Arcs, France, pp. 511–516.
- Thekekara, N. P. (1974), Extraterrestrial solar spectrum, 3000–6100 Å at 1-Å intervals, *Appl. Opt.* 13:518–522.
- Tucker, C. J. (1980), Remote sensing of leaf water content in the near infrared, *Remote Sens. Environ.* 10:23–32.
- Vogelmann, J. E., and Rock, B. N. (1986), Assessing forest decline in the coniferous forests of Vermont using NS-001 Thematic Mapper Simulator data, *Int. J. Remote Sens.* 7:1303–1321.
- Vogelmann, J. E., and Rock, B. N. (1987a), Assessing forest damage in high elevation coniferous forests in Vermont and New Hampshire using Thematic Mapper data, *Remote Sens. Environ.*, forthcoming.
- Vogelmann, A. F., and Rock, B. N. (1987b), Anatomy of red spruce needles from forest decline sites in Vermont, *Environ. Exp. Bot.*, forthcoming.

- Vogelmann, H. W., Bliss, M., Badger, G., and Klein, R. M. (1985), Forest decline on Camels Hump, Vermont, *Bull. Torrey Bot. Club* 112:274–287.
- Wellburn, A. R., and Lichtenthaler, H. K. (1982), Program to calculate the amounts of chlorophyll a and b and total carotenoids from spectral values of plant extracts in different solvents, *Biochem. Microcomput. Users Group Newsletter* 7:22–25.
- Westman, W. E., and Price, C. V. (1987), Remote detection of air pollution stress to vegetation: laboratory-level studies, In *Proceedings of the International Geoscience and Remote Sensing Symposium (IGARSS '87)*, IEEE 87CH2434-9, IEEE, New York, Vol. 1, pp. 451–456.

Received 19 January 1987; revised 28 July 1987